Investigation on the Impact of Protrusion Parameter on the Efficiency of Converting Additional Windage Loss for Ingress Alleviation in Rotor-Stator System

Dongdong Liu
Lead-author
National Key Laboratory of Science and Technology on Aero-Engine Aero-thermodynamics, Beihang University, 37# Xueyuan Road, Haidian District, Beijing, 100191, P. R. China
liudongdongbuaa@buaa.edu.cn

Zhi Tao
Co-author
National Key Laboratory of Science and Technology on Aero-Engine Aero-thermodynamics, Beihang University, 37# Xueyuan Road, Haidian District, Beijing, 100191, P. R. China
tao_zhi@buaa.edu.cn

Xiang Luo[1]
Corresponding author
National Key Laboratory of Science and Technology on Aero-Engine Aero-thermodynamics, Beihang University, 37# Xueyuan Road, Haidian District, Beijing, 100191, P. R. China
xiang.luo@buaa.edu.cn

Wenwu Kang
Co-author
National Key Laboratory of Science and Technology on Aero-Engine Aero-thermodynamics, Beihang University, 37# Xueyuan Road, Haidian District, Beijing, 100191, P. R. China
wenwukang@buaa.edu.cn

Hongwei Wu[2]
Corresponding author
Department of Mechanical and Construction Engineering, Faculty of Engineering and Environment, Northumbria University, Newcastle upon Tyne, NE1 8ST, United Kingdom
hongwei.wu@northumbria.ac.uk

Xiao Yu
Co-author
Shenyang Aero-engine Research Institute, Aviation Industry Corporation of China, Shenyang, 110015, China
yx-mail@sohu.com

---

[1] Xiang Luo, National Key Laboratory of Science and Technology on Aero-Engine Aero-thermodynamics, School of Energy and Power Engineering, Beihang University. Beijing, P. R. China.

[2] Hongwei Wu, Department of Mechanical and Construction Engineering, Faculty of Engineering and Environment, Northumbria University, Newcastle upon Tyne, NE1 8ST, United Kingdom.

Abstract:

This paper presents a detailed investigation on the impact of protrusion parameter including both radial position and amount on the efficiency of cavity with protrusion converting additional windage loss for ingress alleviation in Rotor-Stator system. Experiment is conducted to explore the effect of protrusion parameter on ingress and the corresponding additional windage loss is also calculated. During the experiment rotor-mounted protrusions are circumferentially assembled at three different radial positions (0.9b, 0.8b and 0.7b) each with four different amounts (32, 24, 16 and 8). Measurements of CO_2 concentration and pressure inside turbine cavity are conducted. In the experiment, the annulus Reynolds Number and rotating Reynolds Number are set at 1.77×10^5 and 7.42×10^5 respectively, while the dimensionless sealing air flow rate ranges from 3047 to 8310. Experiment result shows that, the cases of protrusion set at 0.8b achieve higher sealing efficiency than other cases as the cavity pressure is enhanced. The effect of protrusion amount on ingress could be obviously seen when C_W is small or protrusion set in 0.7b. Furthermore, an parameter to evaluate which case obtains higher efficiency of converting additional windage loss for ingress alleviation, or alleviates ingress more efficiently for short, is applied for discussion. It is found the case "C, N=8" alleviates ingress most efficiently among all the cases. Therefore proper setting of the protrusion could lead to high efficiency of converting additional windage loss for ingress alleviation in rotor-stator system.

***Key words**: ingestion; protrusion; experiment; windage loss*

1. INTRODUCTION

In gas turbine, for the purpose of heat transfer enhancement or inevitable structure design, protrusion always exists inside the cavity of gas turbine. It causes

the addition windage loss and alleviation of ingress inside cavity at the same time. The addition windage loss was found and studied by many researchers [1-5], but the alleviation effect of protrusion on ingress was found by Sangan [6] and Liu[7].

The effect of the rotor-mounted cylinder protrusion on hot gas ingestion through rim seal was investigated both experimentally and theoretically by Liu [7]. The orifice model [8, 9] was modified and utilized to explore the ingress mechanism of cavity with protrusion. A new factor, the combination of static pressure and tangential velocity, was introduced to better understand the phenomenon.

However, in order to apply setting protrusion inside cavity for preventing ingress, the side effect of protrusion inside cavity, namely the additional windage loss, should be reduced at maximum extent. In other words, installation of protrusion should be highly effective, i.e. highly enhanced sealing efficiency with least additional windage loss. Otherwise this application would be inefficient and unpractical.

Among the studies of windage loss caused by high rotating rotor [10-15], many researchers found the setting of protrusion on rotor could strengthen the windage loss dramatically and change the cavity flow greatly. It was found the addition windage loss was affected by turbulent flow parameter and geometrical factors such as shape, radial position and amount of protrusion. Zimmermann [2] experimentally measured the friction moment caused by seven type protrusions. It was proposed that the shape of the protrusion impacted the moment of rotor and cover of the protrusion could reduce the friction moment effectively. These characters were also found by Daniels [3] and Luo [1]. In addition, it was told that the distance between

static wall and rotating wall also was an important factor. Long [4] investigated experimentally the impact of the amount and radial position of the protrusion on windage loss and it was shown that the increase of the protrusion amount and radial position resulted in higher windage loss. From the experiment result of Haaser [16], the core flow inside turbine cavity was considered to be a major factor to impact windage loss. All the factors affected the windage loss by changing the turbulent flow parameter inside turbine cavity. Miles [17] used PIV to measure the flow of cavity with protrusion and it was found that the increase of the protrusion size resulted in the increase of the friction moment and tangential velocity of the core flow.

In addition, the protrusions were found to affect each other and made the effect of protrusion on windage loss more complicated. It was found By Zimmermann [2] the ratio of protrusion pitch (distance between protrusions) and protrusion diameter (p/D) was related to the windage loss. When p/D>6, the moment coefficient of rotor increases with the increase of protrusion amount; when p/D<6, the protrusions begin to interact with each other; when p/D<4, the increase of protrusion amount would lead to decrease of moment coefficient of rotor. This phenomenon was also presented in the experiment result of Gartner [4]. Moghaddam [18] numerically increased the protrusion amount from 0 to 60 and found the tangential velocity inside cavity stayed still after it was greater than 45, which was agreed with the experiment result of Millward [19].

It can be concluded that the windage loss introduced by protrusion inside cavity is affected by many factors and their effects were studied and quantified by many

researchers. But their effects on ingress are still unknown.

In this paper, the effects of protrusion parameter both the amount and radial position of the protrusion on efficiency of rotor-mounted protrusion converting additional windage loss for ingress alleviation is investigated experimentally. Based on the experimental result, an evaluation parameter is proposed to evaluate whether one case enhances sealing efficiency more effectively than another case. Then a cavity with protrusion that converts the addition windage loss for ingress alleviation most efficiently, namely high alleviation of ingress with low cost of addition windage loss, could be found among all the cases that tested in the experiment. Concentration of tracer particle, carbon dioxide, and pressure are measured in the experiment. During the experiment, the annulus Reynolds Number and rotating Reynolds Number are set at 1.77×10^5 and 7.42×10^5 respectively, while the dimensionless sealing air flow rate ranges from 3047 to 8310.

2. EXPERIMENTAL APPARATUS AND MEASUREMENT TECHNIQUE

The experiment is conducted in National Key Laboratory Science and Technology on Aero-engine Aero-thermodynamics at Beihang University, Beijing, China. The layout of the experimental system is shown in Fig.1.

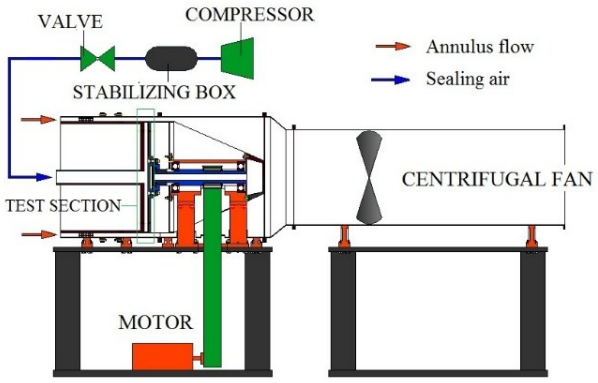

Fig.1 The overall layout of experimental facility

Two kinds of flows are included in the experiment, annulus flow and sealing air. The annulus gas is drawn from atmosphere by a centrifugal compressor (model KF3-95 No6.3E）and enters into the circular channel with 534 mm inner diameter and 574 mm outer diameter. The sealing air is supplied by a 75 kW power compressor and purges into turbine cavity from the center of cavity.

The rotor is driven by a 22 kW DC motor (model Z4-132-2) and its speed can be up to 3000 rpm. The rotating speed is monitored by a photoswitch (model P+F OBT200-18GM60-E5) connecting with tachometer (model YK-23).

2.1 Test Section

The cross section of the test section is illustrated in Fig. 2.

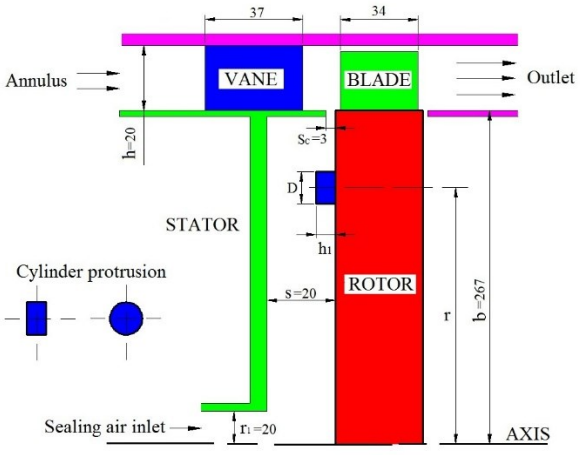

Fig.2 Cross section of overall configuration

There are 59 rotor blades and 32 guide vanes included in annulus. Cylinder rotor-mounted protrusions that are made of aluminum alloy with the height of 6 mm and diameter of 10 mm are circumferentially uniformly assembled on the surface of the rotor disk and rotating with rotor. During the experiment, the protrusions are set in three radial positions, i.e. 0.9b, 0.8b and 0.7b, each with four protrusion amounts, i.e. 32, 24, 16 and 8. Therefore, 12 cases of cavity with protrusion would be tested in the experiment.

For the convenience of description, a naming method is used in this paper. All the cavities with protrusions that tested in the experiment would be named as “model, N=amount of protrusion”. The “model” can be decided from the radial position of protrusion, as shown in Fig. 3.

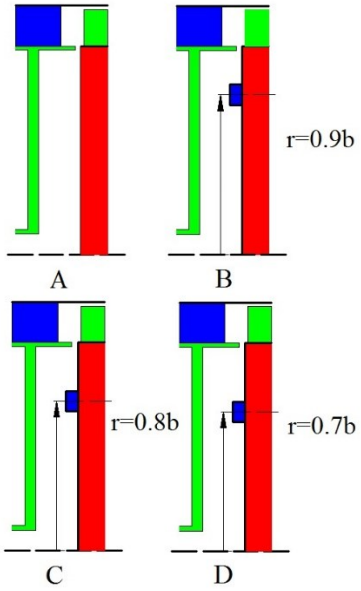

Fig. 3 Structure of four models tested in experiment

It can be found from Fig.3 that cavity without any protrusion is labelled as model A and named as case “A”. It would be tested in the experiment for comparison, while

other cavities with protrusions set in 0.9b, 0.8b and 0.7b are marked as cases of model B, C and D, respectively. Therefore, for the cavity with 32 protrusions setting in 0.9b, it would be labelled as case “B, N=32” in the paper.

2.2 Measurement Technique

2.2.1 Concentration Measurement

In the current study, carbon dioxide is selected as the tracer particle and it is seeded into the sealing air with volumetric concentration around 3% to measure the sealing efficiency inside cavity. The volumetric concentration of the tracer particle is tested by an infrared analyzer (model GXH-3010E). The measurement scope is 0-5.00% and the linear error is ≤±2% FS. The concentration of the annulus flow (c_a), sealing air (c_0) and test positions inside cavity (c) are measured in corresponding positions to obtain the concentration efficiency (ε_c). The concentration sealing efficiency can be calculated by:

$$\varepsilon_c = \frac{c - c_a}{c_0 - c_a} \qquad (1)$$

2.2.2 Mass Flow Rate Measurement

The velocity in annulus is obtained through measurement of the pressure difference between total pressure and static pressure in annulus. A pitot tube is set towards incoming annulus flow to measure the total pressure while the static tube is installed in the corresponding position of the casing to obtain the static pressure. The differential pressure transducer (Rosemount 3051S) with calibration arrangement 0~722.5 Pa is applied to measure the pressure difference. Prior to each test, it is calibrated by the standard wind tunnel, and the uncertainty of the measured velocity

is less than ±2%. The mass flow rate of sealing air is measured by thermal mass flowmeter.

2.2.3 Pressure Measurement

25 time-average static pressure monitors are radially set on the static wall from 0.55b to 1.0b to obtain the radial pressure distribution inside turbine cavity. The differential pressure transducer (Rosemount 3051S) with the calibration arrangement 0~6.216kPa is applied to measure the static pressure. The accuracy of this sensor is ± 0.075 % FS. The uncertainty of the pressure measurement is ± 2 %.

3 DESCRIPTION OF THE EFFICIENCY OF CONVERTING ADDITIONAL WINDAGE LOSS FOR INGRESS ALLEVIATION

When protrusion appears in turbine cavity, it causes additional windage loss which means addition work is converted into cavity. This work results in the increase of total pressure inside cavity and leads to enhancement of sealing efficiency inside cavity. Therefore, it would be the best that all the converted work could be applied for alleviation of ingress, and it would no longer be a kind of loss but a converted benefit for ingress. However, it is impossible for the inevitable flow loss. But it is possible that we could find a specific setting of protrusion inside cavity that could apply high proportion of the converted work (windage loss) for ingress alleviation and reduce the flow loss at maximum extent at the same time. In other words, setting protrusion inside cavity should alleviate ingress efficiently, i.e. with high alleviation of ingress and low cost of addition windage loss.

But which part of the windage loss leads to alleviation of ingress and which part

results in flow loss in turbine cavity is still unknown. The windage loss measurement only indicates the total amount of work converted into turbine cavity but can't identify how much of the work is used for ingress. In this section, the additional windage loss by protrusion would be analyzed theoretically to find which part of the work is useful or useless for ingress. This analysis would be used for further discussion and evaluation of experiment result.

The energy conservation equation for cavity assembled with protrusion could be expressed as below.

$$L_u + q_e = C_p(T_2 - T_1) + \tfrac{1}{2}(V_2^2 - V_1^2) = C_p(T_2^* - T_1^*) \quad (2)$$

Where L_u is the mechanic work converted into cavity flow by protrusion which is the additional windage loss, q_e is the converted heat flux into cavity flow, T^* is the total temperature. The index of 1 and 2 stands for state of cavity flow before and after work adding respectively.

It can be seen in Eq. (2) that the combination of mechanic work and heat flux converted into cavity leads to increase of total enthalpy inside cavity. But there is no heat flux converted into cavity only work in this paper. Therefore some transformations and substitutions would be conducted on Eq. (2) to remove the heat flux and leave the converted work in Eq. (2).

Using the first law of thermodynamics, the equation below could be obtained.

$$q = q_e + L_f = C_p(T_2 - T_1) - \int_1^2 \frac{dp}{\rho} \qquad (3)$$

Where L_f is the lost work due to flow loss. Taking Eq. (3) into Eq. (2) gives

$$L_u = \tfrac{1}{2}(V_2^2 - V_1^2) + \int_1^2 \frac{dp}{\rho} + L_f \qquad (4)$$

As shown in Eq. (4), the additional windage loss caused by protrusion (L_u) is applied for the increase of kinetic energy ($\tfrac{1}{2}(V_2^2 - V_1^2)$), improvement of pressure ($\int_1^2 \frac{dp}{\rho}$) and overcoming the flow resistance (L_f). Assuming the density unchanged, integrating and rearranging Eq. (4) gives

$$L_u = (\tfrac{1}{2}V_2^2 + \frac{p_2}{\rho}) - (\tfrac{1}{2}V_1^2 + \frac{p_1}{\rho}) + L_f \qquad (5)$$

As most of the velocity enhanced is tangential velocity. From the study of Liu [7], we can define $H = \tfrac{1}{2}V^2 + \frac{p}{\rho}$. Therefore, Eq. (5) becomes

$$L_u = H_2 - H_1 + L_f \qquad (6)$$

By Liu, the difference of H between annulus and cavity decides the ingress. From Eq. (6), it can be found that part of the additional windage loss is applied for the increase of H inside turbine cavity ($H_2 - H_1$) and leads to alleviation of ingress, while part of the work is applied to conquer the flow resistance. Based on this, a parameter could be defined to evaluate how much of the additional windage loss is applied for ingress alleviation, or the efficiency of converting additional windage loss for ingress alleviation shown in Eq. (7).

$$\eta = \frac{H_2 - H_1}{L_u} = \frac{\Delta H}{L_u} \qquad (7)$$

Where ΔH is the increment of H inside turbine cavity caused by the protrusion.

4 EXPERIMENTAL RESULT AND DISCUSSION

In this section, the experiment result including the effects of amount and radial

position of protrusion on ingress and cavity pressure are shown in section 4.1, and then in section 4.2 the experiment result would be further analyzed to evaluate the efficiency of converting additional windage loss for ingress alleviation for all cases.

4.1 Experimental Result

4.1.1 The Impact of Amount of Protrusion on Ingress

Fig. 4 shows the radial sealing efficiency for the cases of the same model (model B, C and D) at fixed rotating Reynolds number 7.42×10^5 and annulus Reynolds number 1.77×10^5 and dimensionless flow rate 3047. Each subfigure of Fig.4 shows the comparison of radial sealing efficiencies for the cases of the same model and case "A".

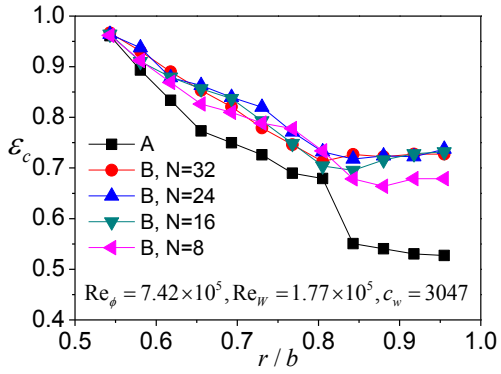

(a) Model B

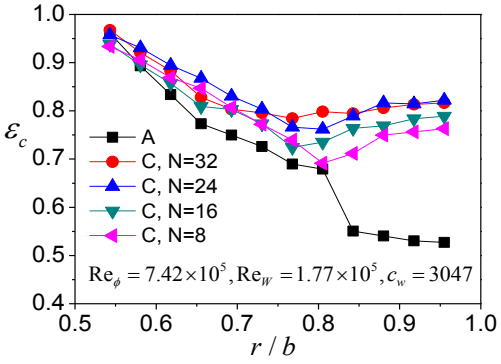

(b) Model C

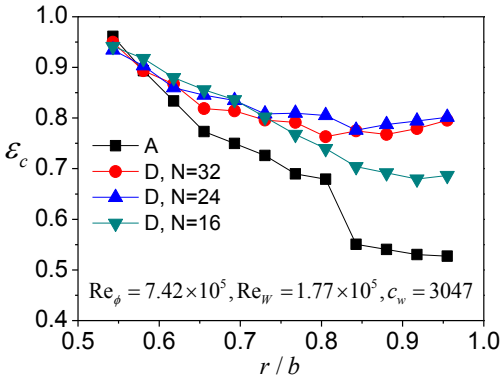

(c) Model D

Fig.4 The radial ε_c for the cases of same model at C_W=3047

The abscissa in Fig. 4 is the dimensionless radius r/b and the ordinate is the sealing efficiency ε_c. Each subfigure in Fig.4 shows the data of case "A" for the purpose of comparison. It can be seen clearly in Fig.4 that ε_c decreases monotonously with the increase of r/b from 0.55b to 0.8b for all cases. But when r/b > 0.8, the character becomes diverse for cases of different models. For the case of model A, there is a sudden drop of ε_c inside cavity and then it becomes even. But ε_c is almost unchanged for the cases of model B and D (as shown in Fig. 4 (a) and (c)), whereas for the cases of model C, ε_c increases slightly with the increase of r/b (as shown in Fig.4 (b)) when r/b > 0.8.

In addition, along with the reduction of the protrusion quantity for the same model, ε_c is unchanged at first, but decreases after it is reduced to a certain quantity. This quantity is different for the cases of the three models. For the cases of model B, ε_c is the same until the amount of protrusion is reduced to 8 which leads to the decrease of ε_c from 0.72 to 0.67 at high radius of cavity (shown in Fig.4 (a)). However, for the cases of model C and D, this decrease of ε_c occurs when the

amount of protrusion is reduced to 16, as illustrated in Fig.4 (b) and (c). It can be concluded that the amount of protrusion can impact the effect of protrusion on ingress but the cases of different models have different characters. This phenomenon could also be found from the experiment result of different C_W as shown in Fig.5. It should be noted that the sealing efficiency measured in r/b=0.96b is chosen to represent the sealing efficiency of cavity.

Fig. 5 presents the variation of ε_c with C_W for the cases of same model (for model B, C and D).

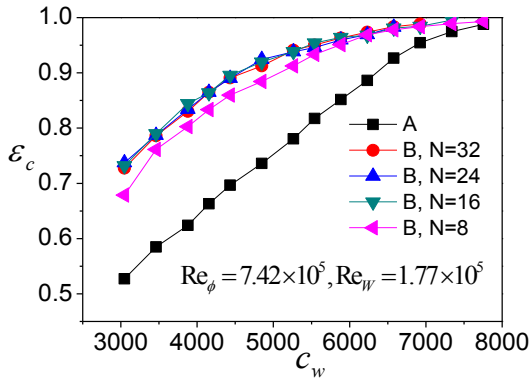

(a) Model B

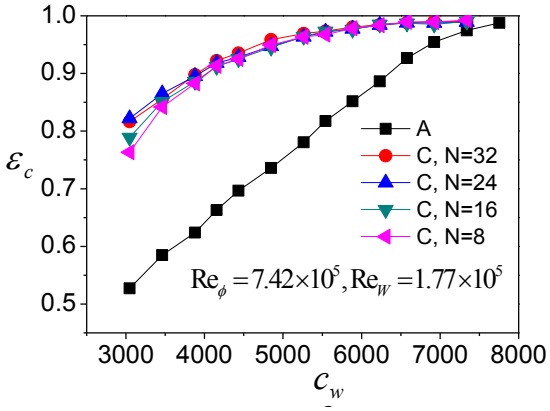

(b) Model C

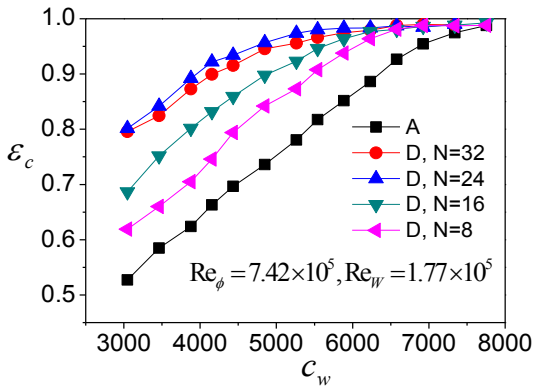

(c) Model D

Fig. 5 The variation of ε_c with C_W for the cases of the same model

It could be observed from Fig. 5 that the sealing efficiency increases with the increase of sealing air flow rate for all cases. With the variation of the protrusion amount, ε_c represents different characteristics for cases of different models. ε_c stays almost the same for the cases of model B and C, whereas it changes for the cases of model D. With the decrease of protrusion number from 32 to 8 for the cases of model D, ε_c at same C_W increases slightly at first and then decreases.

It should be noted that there is a little change of ε_c with the decrease of protrusion amount for the cases of model B and C. At low sealing air flow rates (C_w<6000), ε_c of the case "B, N=8" is lower than that of the other three cases of model B. But ε_c of all the four cases become the same when the C_w > 6000. This situation also could be found for the cases of model C, but the difference of ε_c inside cavity for the four cases only exists when C_W is less than 4000. With the increase of C_W, this difference is reduced and ε_c of all four cases of model C are almost the same.

Therefore, it could be concluded that the reduction of amount of protrusion

couldn't impact ingress when they are assembled in high radius of cavity and with high sealing air flow rate but its impact would be shown when they are set in low radius and with low sealing air flow rate.

4.1.2 The Impact of Radial Position of Protrusion on Ingress

Fig.6 illustrates the comparison of ε_c on static wall for the cases with the same protrusion number (32, 24, 16 and 8) but for different models (model B, C and D) at fixed C_w=3047.

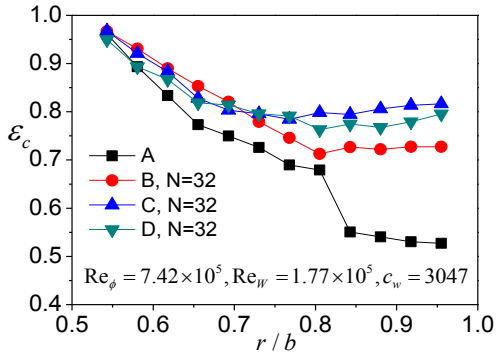

(a) Amount of 32

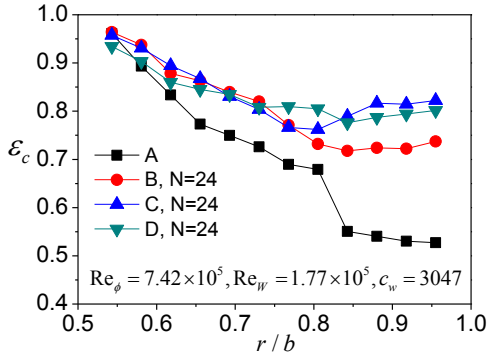

(b) Amount of 24

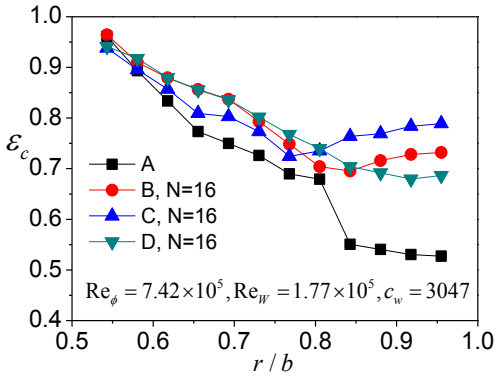

(c) Amount of 16

Fig. 6 The comparison of ε_c for the cases with the same protrusion number at C_W=3047

It can be seen from Fig. 6 that ε_c at low radius of cavity are almost the same for the cases with the same protrusion number. But the difference of ε_c appears at the high radius of cavity. The cases of model C always achieve a higher sealing efficiency than the other cases of the other two models at high radius of cavity. But for cases of model B and D, the cases of model B obtains a higher sealing efficiency than the cases of model D with the protrusion amount of 16 (see Fig. 6 (c)), but ε_c for the cases of model D outweigh that of model B with the protrusion number of 32 and 24, as shown in Fig. 6 (a) and (b). This character could also be found from the experiment result of different C_W as shown in Fig.7. The variation of ε_c with C_W for the cases with same protrusion quantity (32, 24, 16 and 8) are shown in Fig.7.

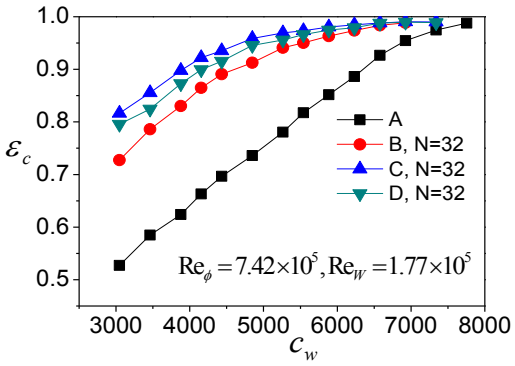

(a) Amount of 32

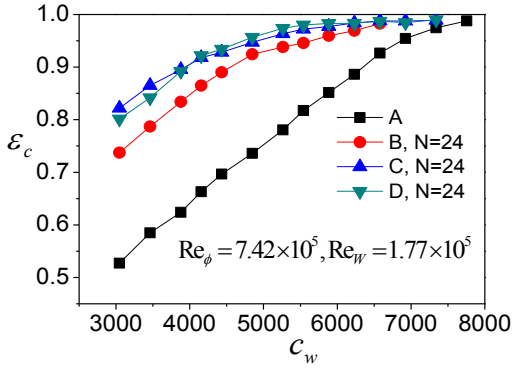

(b) Amount of 24

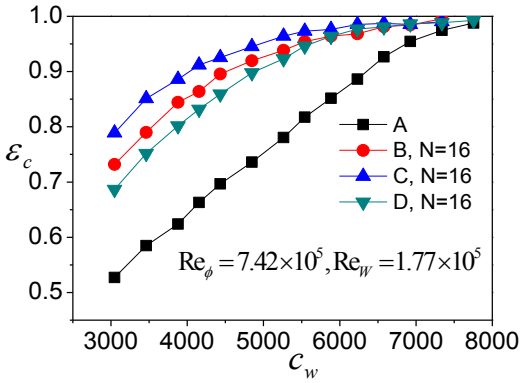

(c) Amount of 16

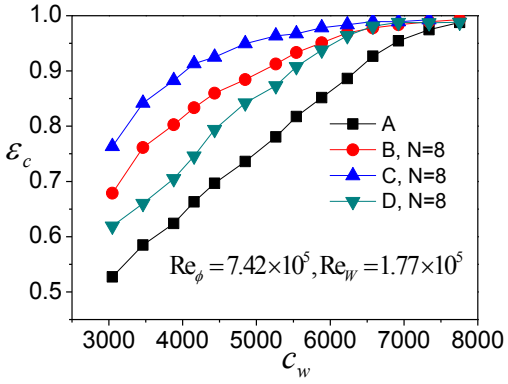

(d) Amount of 8

Fig. 7 The variation of ε_c with C_W for the cases with same protrusion number

It could be seen from Fig. 7 that the cases of model C always obtain the highest sealing efficiency among the cases of all the models. But as shown in Fig. 7 (b), for the cases of the protrusion number fixed at 24, the cases of model C and D achieve almost the same ε_c at different sealing air flow rates. For the cases of model B and D, ε_c of the cases of model B is larger than that of model D when protrusion number is 16 and 8 (see Fig.7 (c) and (d)), while the cases of model D achieve a higher ε_c than that of model B with protrusion number of 32 and 24 (as illustrated in Fig.7 (a) and (b)).

Therefore, the cases of model C achieve higher sealing efficiency than other cases and whether cases of mode B obtain a higher sealing efficiency than the cases of model D depends on protrusion number.

For better understanding the effects of both the protrusion number and radial position on ingress, C_W for all tested cases when ε_c reaches 0.9 are calculated and shown in Fig.8.

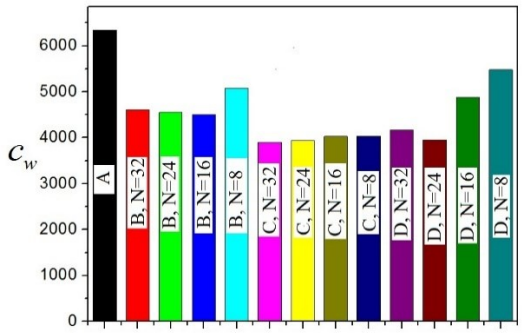

Fig. 8 C_W when sealing efficiency gets 0.9 for all cases

It could be easily found in Fig.8 that the introduction of the protrusion could

effectively alleviate ingress and the protrusion parameter impacts this effect. The cases of model C have an advantage on ε_c than the cases of other models, however the change of protrusion amount causes different characters for different models.

From Fig.8, it seems like that the most effective case that alleviating ingress is the case “C, N=32” as it needs the least amount of sealing air flow rate for the sealing efficiency to get 0.9. But it should be noted that the windage loss that it causes isn’t considered yet. Therefore the most effective case can’t be decided by now.

4.1.3 *The Protrusion Parameter’s Impact on the pressure of turbine cavity*

The flow of cavity with protrusion is analyzed first. Fig. 9 presents the flow of hot gas ingestion with rotor-mounted protrusion.

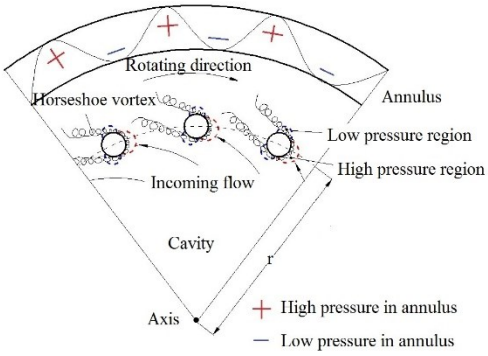

Fig. 9 The flow of hot gas ingestion with rotor-mounted protrusion

The flow of the annulus and cavity when cylinder protrusions are assembled in rotor is schematically shown in Fig. 9. The section flow includes annulus flow and cavity flow. In annulus, circumferentially uneven pressure is generated by vane and blade. In cavity, cavity flow impingings on the cylinder protrusions and causes high and low pressure regions inside cavity, which creates horseshoe vortex at the same time.

As the protrusion is assembled on rotating disk, the rotating protrusion would convert work into cavity flow which would result in the increase of pressure and tangential velocity inside cavity. On the other hand, the flow around circular cylinder generates horseshoe vortex and leads to the flow losses in cavity which would lead to pressure reduction. In addition, the interaction among the horseshoe vortexes and gap vortexes may enhance the flow losses. Therefore, whether the pressure inside cavity can be strengthened by the protrusion depends on the specific condition that whether the work converted into cavity outweighs the flow losses.

The time-average pressure on static wall for four cases when C_w=3047 is measured in experiment and shown in Fig.10.

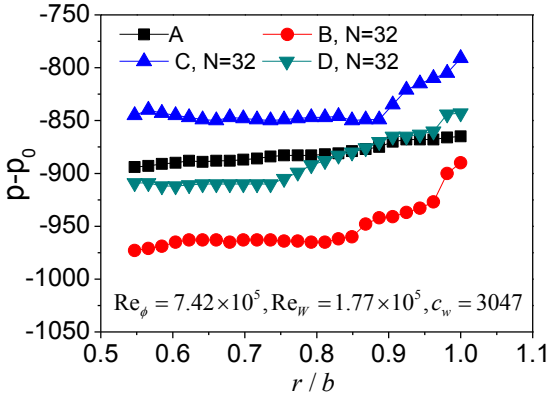

Fig.10The pressure on static wall for four cases when C_W=3047

The abscissa of Fig.10 is the dimensionless radius r/b, and the ordinate is pressure difference of static pressure on static wall (P) and the pressure in annulus inlet (P_0). From Fig.10, it could be found that the pressure of cavity without protrusion (the case “A” in Fig.10) increases monotonously with the dimensionless radius while for the cases of cavity with protrusion the cavity pressure stay still in low radius but increase monotonously with radius in high radius. From the whole figure, it could be

easily seen that the case “C, N=32” achieves the highest pressure inside cavity while the case “B, N=32” has the lowest pressure among these four cases. In other words, it could be interpreted that compared with the cavity without protrusion the cavity pressure is improved by 32 cylinder protrusions assembled in 0.8b but it is reduced by the 32 cylinder protrusions set in 0.9b. This may be attributed to the fact that the protrusions set in 0.9b result in interaction of the ingress flow and horseshoe vortex and lead to much more flow losses than the work the protrusion converted. Therefore, this may be the cause that the cases of model C obtain the highest sealing effect then the cases of the other models for the same amount of protrusions.

4.2 Further Discussion of Experiment result

In this section, the experiment result of ingress is further analyzed by adding the additional windage loss, and the work efficiency η shown in Eq. (7) is applied to evaluation of the efficiency of converting additional windage loss for ingress alleviation for all the cases tested in the experiment.

The empirical formula of additional moment induced by protrusion proposed by Coren [20], shown in Eq. (8), would be utilized in this paper to calculate the additional windage loss by protrusion, L_u.

$$C_m = C\left(0.115 C_w^{0.47} Re_{\Phi}^{-0.3504} \frac{r_b^{0.34}}{p} - 0.00179\right) \quad (8)$$

Where C_m is the moment coefficient ($C_m=M/(0.5\rho\omega^2 b^5)$, M is the rotor moment), r_b is the radius of protrusion and p is the pitch between protrusions. The additional windage loss can be expressed as

$$L_u = M \times \omega = C_m \times 0.5\rho\omega^3 b^5 \quad (9)$$

L_u can be obtained from Eq. (9) and (10). But it is hard to get ΔH of Eq. (7). Therefore, η would not be calculated in this paper, instead an alternative parameter is proposed to evaluate whether one case applies the converted work more efficient than other one. In other words, we would find an expression that can indicate relative magnitudes of $\frac{\eta_1}{\eta_2}$ which is shown in Eq. (10).

$$\frac{\eta_1}{\eta_2}=\frac{\Delta H_1}{L_{u,1}}\Big/\frac{\Delta H_2}{L_{u,2}} \qquad (10)$$

The description of this parameter includes three cases. Case 0 is the cavity without any protrusion, while case 1 and 2 are the cavities with protrusion but with different parameters. The variation of sealing efficiency with sealing air flow rate for these three cases are shown in Fig.11.

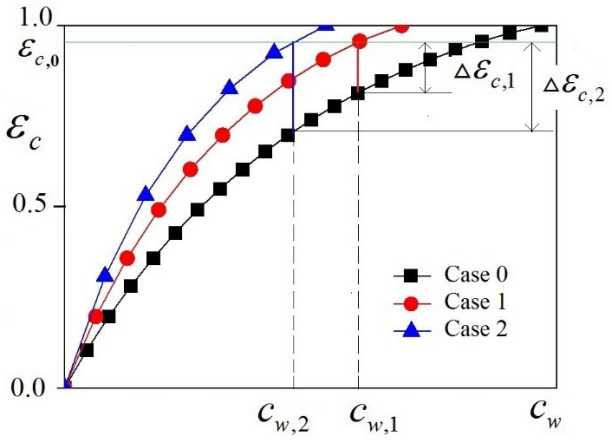

Fig.11 The variation of ε_c with C_W for three cases

From Fig.11 it can be seen that case 1 and 2 have different increments of sealing efficiency compared with case 0. The green line is $\varepsilon_c=\varepsilon_{c,0}$. In the circumstance, it is assumed that $\varepsilon_c=\varepsilon_{c,0}$ is the goal that is to be achieved in cavity with purged air. The vertical lines (red and blue lines) start from the intersection of $\varepsilon_c=\varepsilon_{c,0}$ and sealing

efficiency curves to sealing efficiency curve of case 0 give the increments of sealing efficiencies from case 0 to case 1 and 2, □ and□ respectively, at corresponding sealing air flow rates shown in ordinate, $C_{w,1}$ and $C_{w,2}$.

With $C_{w,1}$ and $C_{w,2}$, the addition works converted into cavity can be obtained from Eq. (8), which are set as $L_{u,1}$ and $L_{u,2}$ for case 1 and 2 respectively. While □ and□ could be used to represent the relative magnitudes of ΔH for case 1 and 2, respectively, as the increase of H inside cavity (ΔH) leads to increase of sealing efficiency (□). Therefore, the relative magnitudes of $\Delta H_1 / \Delta H_2$ can be indicated by □ □. As the rotating speed of rotor is set at a constant value in this paper, then $L_{u,1} / L_{u,2} = C_{m,1} / C_{m,2}$. Therefore the expression: $\square / \square$ could be used to indicate the relative magnitudes of $\frac{\eta_1}{\eta_2} = \frac{\Delta H_1}{L_{u,1}} \Big/ \frac{\Delta H_2}{L_{u,2}}$.

By choosing one of the cases as a constant reference (with subscript 0), we defines an evaluation parameter δ to indicate whether one case increases sealing efficiency more efficiently than another cases, as shown in Eq. (11).

$$\delta = \square / \qquad (11)$$

In this paper, the case “C, N=32” is chosen as the constant reference and $\varepsilon_c = 0.9$ is the sealing efficiency expected to achieve in cavity. Therefore, if one case has a δ higher than 1, it means its setting of protrusion alleviates ingress more efficiently than the case “C, N=32”. At the same time, if one case has a higher δ than the other case, it means it applies the converted work more efficiently than the other case. Fig. 12 shows the δ for all the cases.

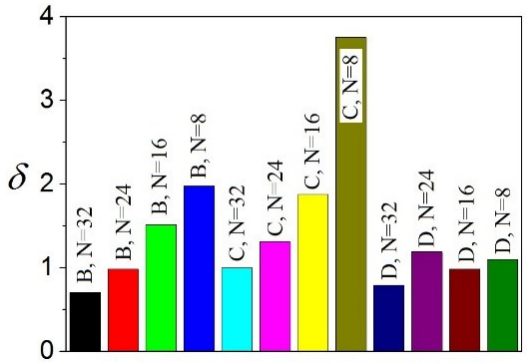

Fig. 12 the δ for all the cases

It can be seen in Fig.12 for the cases of model B and C, the δ increase with the decrease of protrusion quantity while for the cases of model D the reduction of protrusion number doesn't lead to increase of δ. It can be clearly found in Fig.12 that the case "C, N=8" achieves the highest δ among all the cases tested in the experiment. Compared with Fig. 8, although case "C, N=32" alleviates ingress the most, it causes too much additional work. Therefore the case "C, N=8" highly improves the sealing efficiency with least addition work. In other words, it converts the additional windage loss for ingress alleviation most efficiently among all the cases.

From Fig.12, it can be concluded that with properly setting of protrusion, high sealing efficiency and low windage loss can be obtained at the same time. In the condition of this paper, setting 8 protrusions in 0.8b could convert the additional windage loss for ingress alleviation most efficiently.

5 CONCLUSIONS

In this paper, the effect of protrusion parameter including amount and radial position on the efficiency of turbine cavity with protrusion converting additional windage loss for ingress alleviation is investigated experimentally.

The effect of protrusion parameter on ingress is measured in experiment. The experiment result shows the cases of model C achieve higher sealing efficiency than other cases. While whether the case of model D outweighs that the case of model B depends on the amount of protrusion. The effect of protrusion amount on ingress could be obviously seen when protrusion is set in low radius position or sealing air flow rate is small.

The effect of protrusion parameter on turbine cavity pressure is also explored. The cases of model C enhance the cavity pressure while other cases do not. It is considered to be the reason that the cases of model C achieve a higher sealing efficiency than that of other models.

In the further discussion, the accompanied windage loss by protrusion is taken into consideration to compare the efficiency of converting additional windage loss for ingress alleviation for all the cases. The case “C, N=8” is found to alleviate ingress most efficiently among all the cases as it alleviates ingress greatly and costs low windage loss at the same time. It is concluded that proper arrangement of protrusions would lead to less windage loss and high sealing efficiency at the same time and result in high efficiency of converting additional windage loss for ingress alleviation.

ACKNOWLEDGMENT

The authors gratefully acknowledge the financial support from the National Natural Science Foundation of China (No. 50806004), the Carnegie Trust for the Universities of Scotland (No. 31729) and the Innovation Foundation of BUAA for PhD Graduates.

NOMENCLATURE

b	radius of disk
c	carbon dioxide concentration
c_0	the carbon dioxide concentration of sealing air
C_m	the moment coefficient ($C_m=M/(0.5\rho\omega^2 b^5)$)
C_W	non-dimensional flow rate [$=\dot{m}$]
c_a	the carbon dioxide concentration of annulus flow
D	diameter of cylinder protrusion
G_c	seal clearance ratio ($=s_c/b$)
h	height of annulus path
H	Combination of pressure and velocity($=\frac{1}{2}V^2+p/\rho$)
ΔH	The increment of H inside cavity by protrusion
h_1	height of cylinder protrusion
L_u	the addition windage loss caused by protrusion
L_f	the flow resistance
M	the rotor moment

$\dot{m}$	mass flow rate
$\dot{m}_c$	mass flow rate of sealing air
p	static pressure, pitch
p_0	annulus pressure at inlet
q_e	the converted heat flux into cavity flow
r	radius
r_1	radius of sealing air inlet
r_b	the radius of protrusion
Re_W	annulus Reynolds number [$=\rho W b/\mu$]
Re_ϕ	rotational Reynolds number[$=\rho\Omega b^2/\mu$]
s	axial clearance between rotor and stator
s_c	seal clearance
T^*	total temperature
V	velocity
V_ϕ	tangential velocity
δ	Evaluation parameter [=(
ε_c	concentration sealing effectiveness [$=(c-c_a)/(c_o-c_a)$]
Δ	the increment of sealing effectiveness
η	efficiency of mechanic work[$=(H_2-H_1)/L_u$]
μ	dynamic viscosity
υ	kinematic coefficient of viscosity
ρ	density

ω	rotating velocity
Ω	rotating velocity of disk

Subscripts

a	annulus
in	incoming flow
o	sealing flow
0,1,2	mathematic variable

REFERENCES

[1] X. Luo, D. Zhang, Z. Tao, G.-Q. Xu, Q.-S. Wang. Windage Measurements in a Rotor-Stator System with Superimposed Cooling and Rotor-Mounted Protrusions. Journal of Engineering for Gas Turbines and Power, 2014, 136(4): 042505.

[2] H. Zimmermann, A. Firsching, G. H. Dibelius, M. Ziemann, 1986, “Friction Losses and Flow Distribution for Rotating Disks with Shielded and Protruding Bolts”, J. Eng. Gas turbines power, Vol. 108, pp. 547-552.

[3]W. A. Daniel, B. V. Johnson, D. J. Graber, 1991, “Aerodynamic and Moment Characteristics of Enclosed Co/Counter-Rotating Discs”, J. Turbomach., Vol. 113, pp.67-74.

[4] C. A. Long, A. L. Miles, D. D. Coren, 2012, “Windage Measurements in a Rotor Stator Cavity with Rotor Mounted Protrusions and Bolts”, ASME Paper GT2012-69385.

[5]W. Gartner, 1998, “A Momentum Integral Method to Predict the Frictional Moment of a Rotating Disc with Protruding Bolts”, ASME Paper 98-GT-138.

[6]C. M. Sangan, J. A. Scobie, J. M. Owen, G. D. Lock, K. M. Tham, V. P. Laurello, 2014, “Performance of a Finned Turbine Rim Seal”, J. Turbomach. Vol. 136:111008-1 to 10.

[7]D.-D. Liu, Z. Tao, X. Luo, H.-W. Wu and X. Yu, 2016, “Development of a New Factor for Hot Gas Ingestion through Rim Seal”, J. Eng. Gas Turbines Power, Vol. 138:072501-1 to 10.

[8]J. M. Owen, 2011, “Prediction of Ingestion Through Turbine Rim Seals—Part I: Rotationally Induced Ingress”, J. Turbomach., Vol. 133:031005-1 to 9.

[9]J. M. Owen, 2011, “Prediction of Ingestion Through Turbine Rim Seals—Part II: Externally Induced and Combined Ingress”, J. Turbomach. Vol. 133:031006-1 to 9.

[10]Owen J. M., 1989, “An approximate solution for the flow between a rotating and a stationary disk”, Journal of Turbomachinery, 111(3): 323-332.

[11]Bayley F. J., Owen J. M., 1970, “The fluid dynamics of a shrouded disc system with a radial outflow of coolant”, Journal of Engineering for Power, Vol.92: 335-341.

[12]Mochizuki S., Yang W. J., 1986, “Flow friction on co-rotating parallel-disk assemblies with forced through-flow”, Experiments in fluids, 4(1): 56-60.

[13]Itoh M., Yamada Y., Imao S., et al., 1992, “Experiments on turbulent flow due to an enclosed rotating disk”, Experimental thermal and fluid science, Vol.5: 359-368.

[14]Kang J. S., Cha B. J., Ahn I. K., 2008, “Modeling and experimental evaluation on torque loss in turbine test rig”, ASME paper, GT1079-1085.

[15]Coren D., Childs P. R. N., Long C. A., 2009, “Windage sources in smooth-walled rotating disc systems”, Proceedings of the Institution of Mechanical Engineers, Part C: Journal of Mechanical Engineering Science, Vol.223: 873-888.

[16]Haaser F., Jack J., McGreehan W., 1988, “Windage rise and flowpath gas ingestion in turbine rim cavities”, Journal of engineering for gas turbines and power, Vol.110: 78-85

[17]A. L. Miles, 2012, “An Experimental Study of Windage Due to Rotating and Static Bolts in an Enclosed Rotor-Stator System”, Brighton: University of Sussex.

[18]Moghaddam E. R., Coren D., Long C. A. and Sayma A., 2011，“A numerical investigation of moment coefficient and flow structure in a rotor-stator cavity with rotor mounted bolts”, ASME paper, GT2011-45588

[19]Millward J. A., Robinson P. H., 1989, “Experimental investigation into the effects of rotating and static bolts on both windage heating and local heat transfer coefficients in a rotor/stator cavity”, American Society of Mechanical Engineers.

[20]Coren D., 2007, “Windage due to protrusions in rotor-stator systems”, Brighton: University of Sussex.

Figure Captions List